Research Square

Preprints are preliminary reports that have not undergone peer review.
They should not be considered conclusive, used to inform clinical practice,
or referenced by the media as validated information.

Model for prediction of film composition in the DC Magnetron Sputtering of Fe-Cr-Ni-Mn-Cu and Al-Fe-Cr-Ni-Cu High-Entropy Alloys

Liviu Badea

liviu9badea@gmail.com

National Research and Development Institute of Non-Ferrous and Rare Metals

Alexandru Okos

National Research and Development Institute of Non-Ferrous and Rare Metals

Marian Nicolae Costea

National Research and Development Institute of Non-Ferrous and Rare Metals

Arcadii Sobetkii

National Research and Development Institute of Non-Ferrous and Rare Metals

Laurentiu Florin Mosinoiu

National Research and Development Institute of Non-Ferrous and Rare Metals

Dumitru Mitrica

National Research and Development Institute of Non-Ferrous and Rare Metals

Ana Maria Mocioiu

National Research and Development Institute of Non-Ferrous and Rare Metals

Laura Madalina Cursaru

National Research and Development Institute of Non-Ferrous and Rare Metals

Article

Keywords: DC magnetron sputtering, High-entropy alloys (HEA), Preferential sputtering, Yamamura-Tawara sputtering yield, Thin film composition

Posted Date: September 3rd, 2026

DOI: https://doi.org/10.21203/rs.3.rs-10727027/v1

License: This work is licensed under a Creative Commons Attribution 4.0 International License.
Read Full License

Additional Declarations: No competing interests reported.

Model for prediction of film composition in the DC Magnetron Sputtering of Fe-Cr-Ni-Mn-Cu and Al-Fe-Cr-Ni-Cu High-Entropy Alloys

Liviu Badea[1+*], Alexandru Okos[1+], Marian Nicolae Costea[1+], Arcadii Sobetkii[1], Laurentiu Florin Mosinoiu[1], Dumitru Mitrica[1], Ana Maria Mocioiu[1], Laura Madalina Cursaru[1].

[1]National Research and Development Institute of Non-Ferrous and Rare Metals, 178-184 Biruintei Blvd, 077145 Pantelimon, Romania; lbadea@imnr.ro (L.B.); alexandru.okos@imnr.ro (A.O.); mcostea@imnr.ro (M.N.C.); arcadii@imnr.ro (A.S.); lmosinoiu@imnr.ro (L.F.M.); dmitrica@imnr.ro (D.M.); ammocioiu@imnr.ro (A.M.C.); mpopescu@imnr.ro (L.M.C.)

Abstract

The paper proposes an algorithmic model that explains compositional transfer in DC magnetron sputtering of two families of high-entropy alloys (HEAs): Fe-Cr-Ni-Mn-Cu and Al-Fe-Cr-Ni-Cu. It considers the Yamamura-Tawara composition-dependent sputtering yields, cascade correction for multicomponent films, iterative steady-state preferential sputtering, and eight empirically determined growth factors of the film. The compositions of targets were found from the analysis of cast ingots by chemical means. Copper is predicted to have the maximum and nickel the minimum yield in both cases. Deviations of the target composition from the calculated composition of the film are always lower in Al-Fe-Cr-Ni-Cu as compared to Fe-Cr-Ni-Mn-Cu owing to larger surface binding energy and the absence of manganese, which binds less strongly to the surface. Deviations from the target compositions in both cases are small ±1 wt%, which corresponds to the normal analytical errors of the chemical characterization method (ICP-OES). The modelled composition of the deposited film showed good agreement with the experimental values.

Keywords: DC magnetron sputtering, High-entropy alloys (HEA), Preferential sputtering, Yamamura-Tawara sputtering yield, Thin film composition

1. Introduction

The concept of high-entropy alloys (HEAs) was established in the year 2004 due to separate research by Yeh et al. [1] and Cantor et al. [2]. It was shown that alloys containing at least five principal components have high configurational entropy leading to solid solution formation. Due to the lattice distortion, low atomic diffusion, and synergistic cocktail effect, HEAs possess unique set of properties, reviewed by Miracle and Senkov [3] and George et al. [4].

DC magnetron sputtering technique has become one of the most common methods of depositing HEA thin films of nanocrystalline structure [5]. Possible applications are related to protective hard films and biomedical devices using Fe-Cr-Ni-based alloys' corrosion resistance in combination with antimicrobial properties of Cu [5]. This paper deals with compositions including five elements: Fe-Cr-Ni-Mn-Cu, where both Cu and Mn are used, as well as alloy Al-Fe-Cr-Ni-Cu in which Mn is replaced by Al.

Multicomponent composition obtained by sputtering process is limited by selective erosion of less strongly bound atoms. For the simulation of the process, several methods can be used: Sigmund's cascade theory [6] and Yamamura-Tawara yield formula [7], supported by Bohdansky threshold effect [8]. For HEA target application, one could take into account cascade correction coefficients, found by means of Monte Carlo simulations [9]. Steady state enrichment of surface under bombardment has been examined by Nastasi et al. [10].

In the paper, four alloy compositions are used in the modeling process, for deposition in equal conditions (300 W power, 0.2 Pa pressure), on glass substrates. Parameters of plasma are considered based on the work by Lieberman and Lichtenberg [11]; film characteristics are estimated according to Thornton zone model [12]. Eight semi-empirical factors describe composition modification during transport and growth process. Experimental deposition results were matched to the modelling results.

2. Methodology

The modelling method is a seven-block physics-based semi-empirical computational model, that simulates the transfer of composition in the DC magnetron sputtering process, where the composition of the obtained film is calculated according to the composition of the target and the sputtering efficiencies of each element, adjusted with factors that take into account how the particles move in the plasma, such as diffusion in argon gas and the influence of atomic mass, and the final result is obtained by normalizing the atomic fluxes of all types of particles. The Yamamura-Tawara equation, which was initially developed for monatomic targets, has been further developed by using the SRIM multicomponent cascade correction factor (Kmc), based on data available from literature. The eight semi-empirical correction factors have been assumed to be constant, without conducting any sensitivity study. No consideration has been made about microstructural influence,

poisoning of the target, or angular distribution of fluxes. Gas-phase transport has been simulated through an interpolation technique for the Knudsen number instead of using DSMC techniques.
The proposed alloys were prepared experimentally in a Linn MFG-30 induction furnace, under vacuum and in an inert argon atmosphere. The resulting ingots were subjected to grinding and cutting to obtain the targets used in the magnetron sputtering process.
The thin film depositions were performed on a hybrid PVD (Physical Vapor Deposition) system, using a DC/RF Magnetron Sputtering module manufactured by Kurt J. Lesker, equipped with a 2-inch TORUS circular cathode and a PD500x DC power supply with a maximum power of 1500 W.
Quantitative chemical analysis of targets and thin films was performed using an inductively coupled plasma optical emission spectrometer (ICP-OES), used to determine elemental concentrations in samples by measuring the intensity of radiation emitted by excited atoms in argon plasma.

3. Results and Discussion

3.1 Modelling of Fe-Cr-Ni-Mn-Cu system-based alloys.

From the obtained composition spectrum shown in Fig. 1, one can conclude that the target ordering Mn > Fe > Ni > Cr > Cu, which was established in the simulation of the film composition, was not violated. In particular, the decrease in the content of manganese is maximal—approximately 1 wt %, while iron, nickel, and chromium are enriched by nearly the same amount, which amounts to 0.3–0.4 wt %. This is explained by the fact that manganese, having the minimum surface binding energy (2.98 eV) out of all five metals, evaporates from the surface disproportionately more intensively [7]. Despite being the metal with the maximum sputtering yield in the present case, copper showed the minimal deviation due to the relatively small concentration in the target [9]. The similar increase in the concentrations of the other metals (Fe, Ni, Cr) indicates an even distribution of the sputtered atoms between these metals. This behavior is typical of systems where the main components have similar surface binding energies and atomic masses [10].

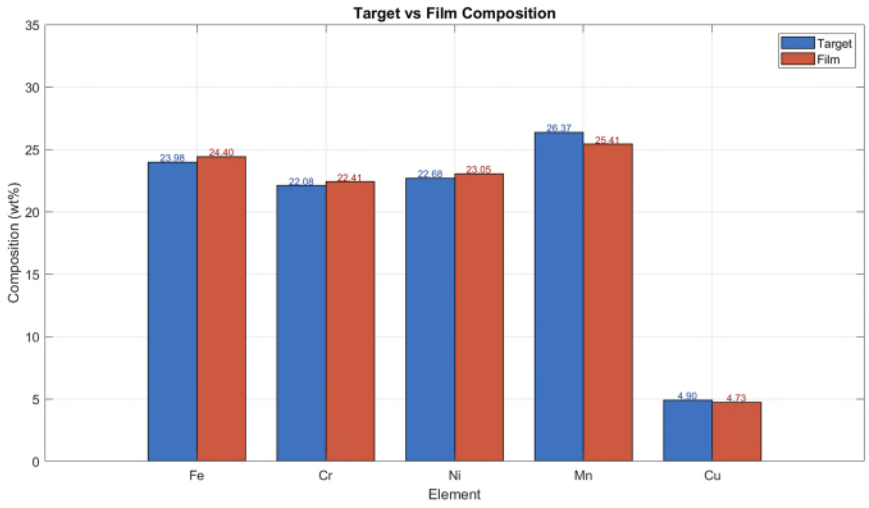


Fig. 1. Comparison between target and predicted film compositions for the Fe-Cr-Ni-Mn-Cu alloy (I8-6) under DC magnetron sputtering conditions.

The profile of composition difference between the target and the film (ΔC_{mod}), illustrated in Figure 2, depicts the above-mentioned changes. The manganese part forms the largest portion of the graph, reaching up to halfway towards the dashed line of reference. The three elements that have been enriched show bars of about equal heights.

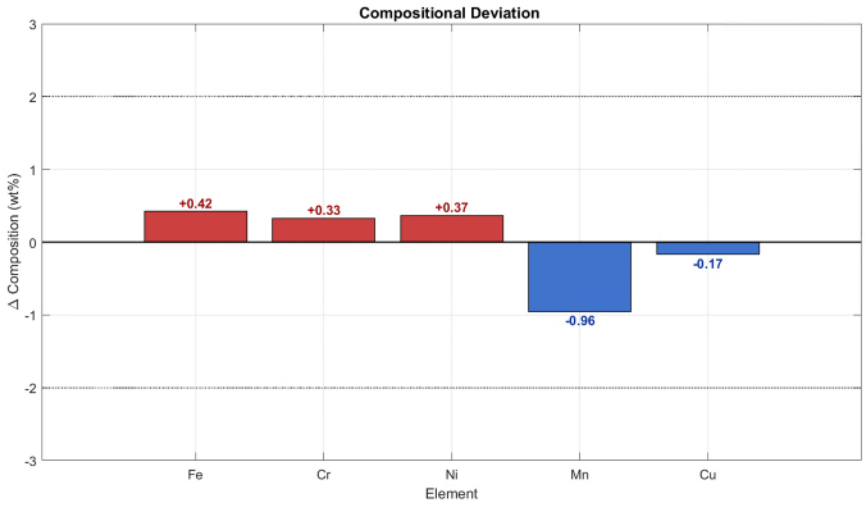


Fig. 2. Element-specific compositional deviations between target and predicted film compositions for the Fe-Cr-Ni-Mn-Cu alloy (I8-6). Positive values indicate enrichment and negative values indicate depletion.

As compared to I8-6, the second composition (Fig. 3) contains roughly twice as much Cu but less Mn. However, despite this major difference in stoichiometry, the same trend can be observed for this composition profile: the ranking order of all five components has not changed and, accordingly, Fe, Cr, and Ni still have a small positive shift in concentration. Thus, this suggests that the enrichment of these three components is determined by the alloy's binding energy rather than the Cu/Mn ratio. The modification of stoichiometry influences the ΔC_{mod} profile (Fig. 4) and leads to a change in the Mn content from -0.96 to -0.82 wt%, which corresponds to its lower concentration initially. As for the Cu content, it changes from -0.17 to -0.34 wt%. This change is proportional to the initial content. Enrichment of the above-mentioned elements, however, has not been modified. In practical terms, changing the ratio of Cu and Mn results in redistribution of the "load" between these two elements, which can be very convenient when designing an alloy due to their different purposes.

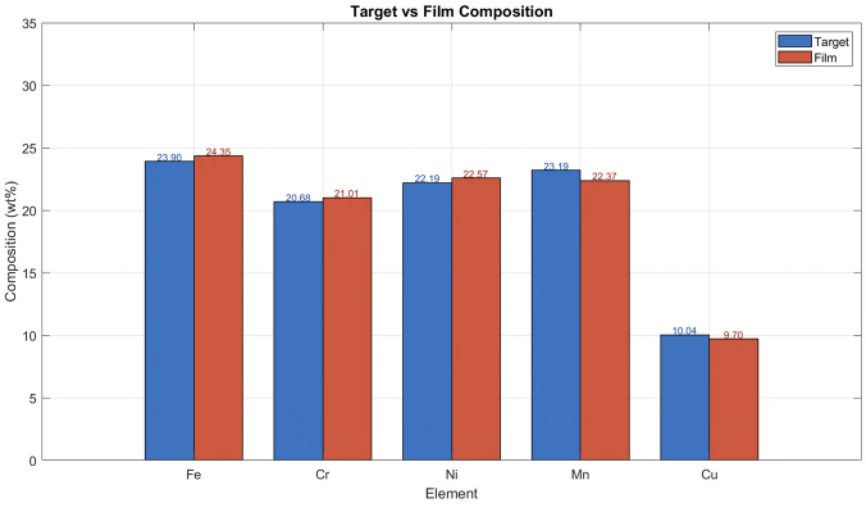


Fig. 3. Comparison between target and predicted film compositions for the Fe-Cr-Ni-Mn-Cu alloy (I8-7) under DC magnetron sputtering conditions.

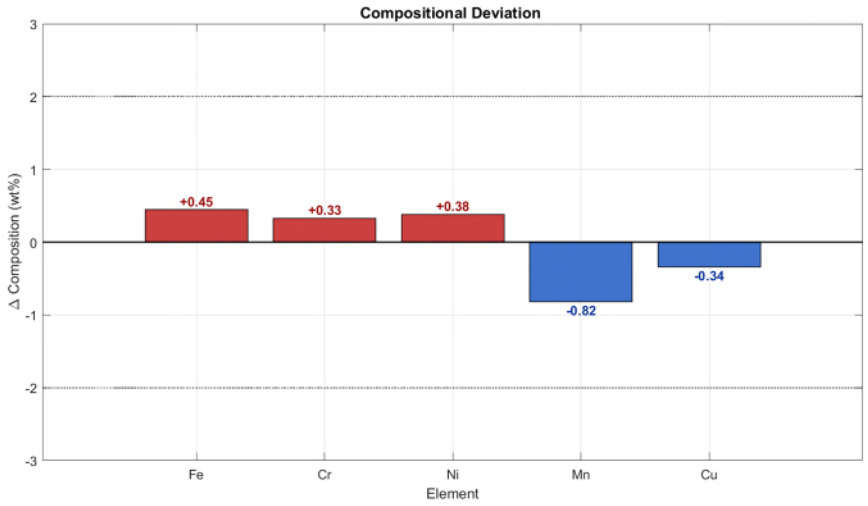


Fig. 4. Element-specific compositional deviations between target and predicted film compositions for the Fe-Cr-Ni-Mn-Cu alloy (I8-7). Positive values indicate enrichment and negative values indicate depletion.

3.2. Sputtering Yield for Fe-Cr-Ni-Mn-Cu system

The radial yield curves shown in Figure 5 explain the above-mentioned discrepancies. The Kinetic molecular components (K_{mc}) corrections used for this analysis (Fe: 1.00, Cr: 1.05, Ni: 0.87, Mn: 0.77, Cu: 1.10), taken from SRIM publications [7], [9] and not calculated here, result in the following element order Cu > Mn > Cr > Fe > Ni along the full radial profile of the target. The peaks of all profiles are observed at the racetrack position (r = 17.5 mm), where the energy of the incident ions is maximal [11]. The leading position of the Cu element is determined by its higher atomic weight, surface binding energy, and Kmc values. The ratio between the yield of Cu and Ni (≈ 1.7:1) is nearly constant throughout the radial profile. Near the edges of the targets, the profiles converge since the energies of ions get close to the Bohdansky cut-off energy [8].

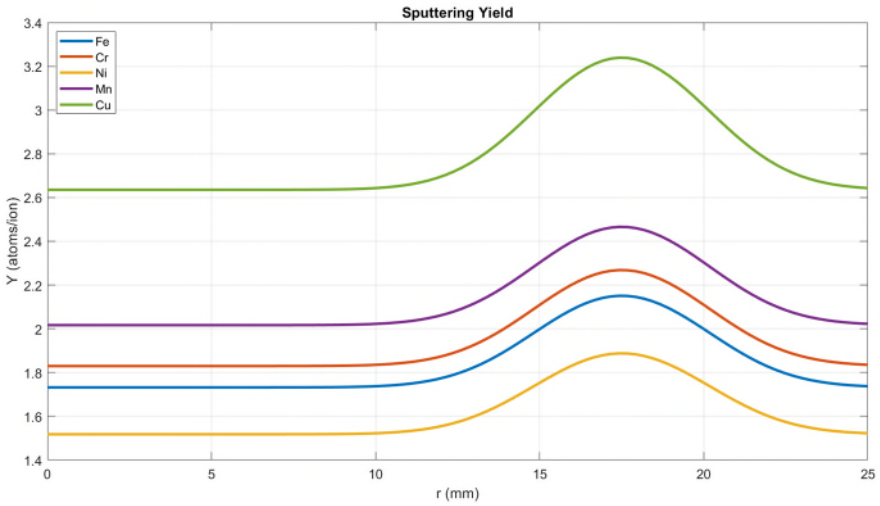


Fig. 5. Radial distribution of element-resolved sputtering yields in the Fe-Cr-Ni-Mn-Cu alloy at ion incidence.

3.3. Modelling of Al-Fe-Cr-Ni-Cu system-based alloys.

A different qualitative pattern of deviation occurs in the Al-Fe-Cr-Ni-Cu case. The target and film bars of Fe, Cr, and Ni practically coincide in Fig. 6, with only a difference in bar height visible for Al and Cu. As seen in Fig. 7, Fe, Cr, and Ni show deviations close to zero, whereas Al and Cu show small but non-zero deviations towards the positive and negative direction, respectively. Thus, this outlier case is quite opposite from that for Fe-Cr-Ni-Mn-Cu diagrams (Figs. 2 and 4), having two rather than one outlier element. This is explained by higher binding energies in this system, leading to smaller spread of yield values and lower driving forces for preferential removal. Fe and Cr have shown the lowest deviation between their content in films and target [10].

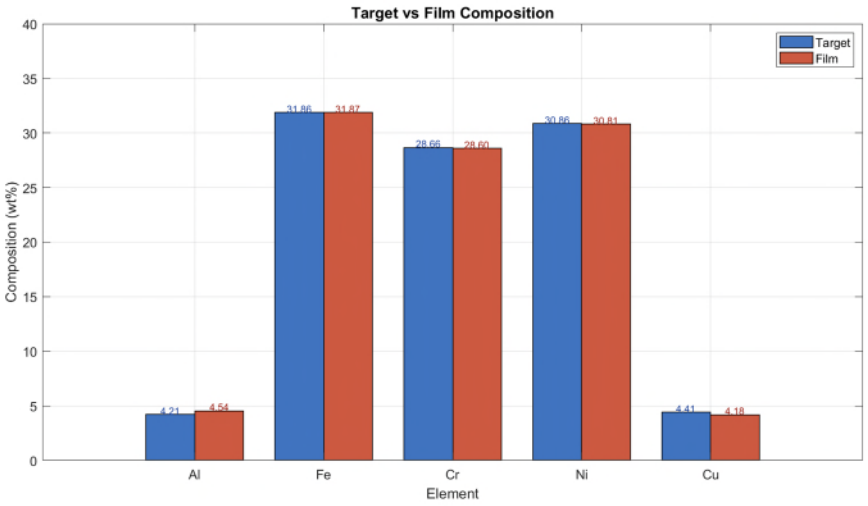


Fig. 6. Comparison between target and predicted film compositions for the AlFeCrNiCu alloy (I8-10) under DC magnetron sputtering conditions.

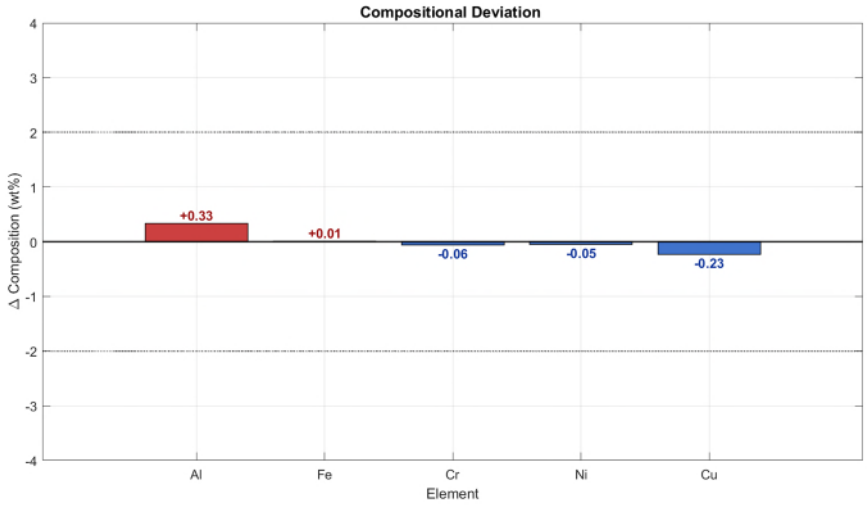


Fig. 7. Element-specific compositional deviations between target and predicted film compositions for the Al-Fe-Cr-Ni-Cu alloy (I8-10). Positive values indicate enrichment and negative values indicate depletion.

Ingot I8-11 is the most compositionally unbalanced one studied here, as Fe accounts for almost 50% of the alloy content while Cr is decreased to approximately 4.5 wt%. Such large asymmetry places this alloy far from equimolar compositions that would correspond to maximal configurational entropy and serves as a relevant example to investigate the model's behavior under non-equimolar stoichiometries. As seen in Fig. 8, the majority of alloying elements Fe and Ni (together accounting for more than 80 wt%) show virtually no shift, as illustrated by insignificant differences in bar heights. Cu, however, shows the largest bar height difference (0.6 wt%) that is about 2.5 times larger than in the case of I8-10, correlating with a three-fold increase of its initial content. This scaling factor can be explained by the assumption that the Cu reduction depends on its absolute flux to the sample surface rather than on changes in the yield efficiency. The ΔC_{mod} plot in Fig. 9 displays only a single significant value related to Cu, while deviations of other four elements do not exceed experimental uncertainties. Interestingly enough, the maximum deviation (0.57 wt%) is less than the smallest Mn contribution observed in Fe-Cr-Ni-Mn-Cu alloys (0.82 wt.%).

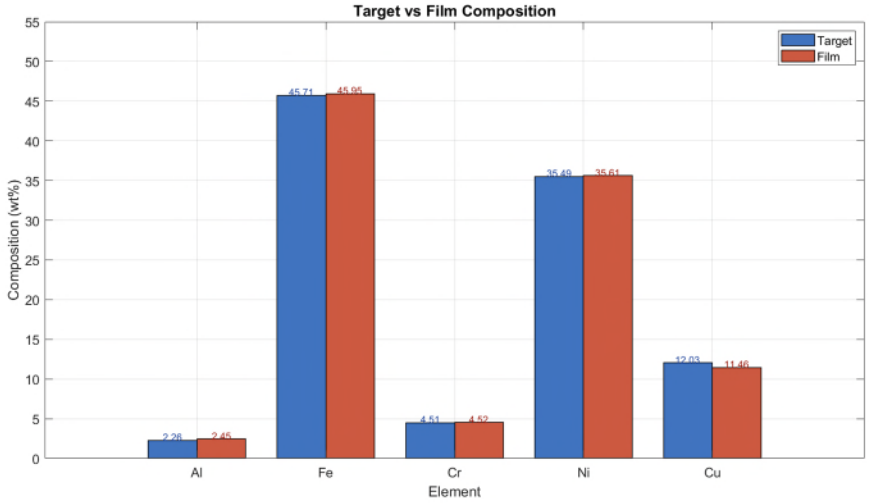


Fig. 8. Comparison between target and predicted film compositions for the AlFeCrNiCu alloy (I8-11) under DC magnetron sputtering conditions.

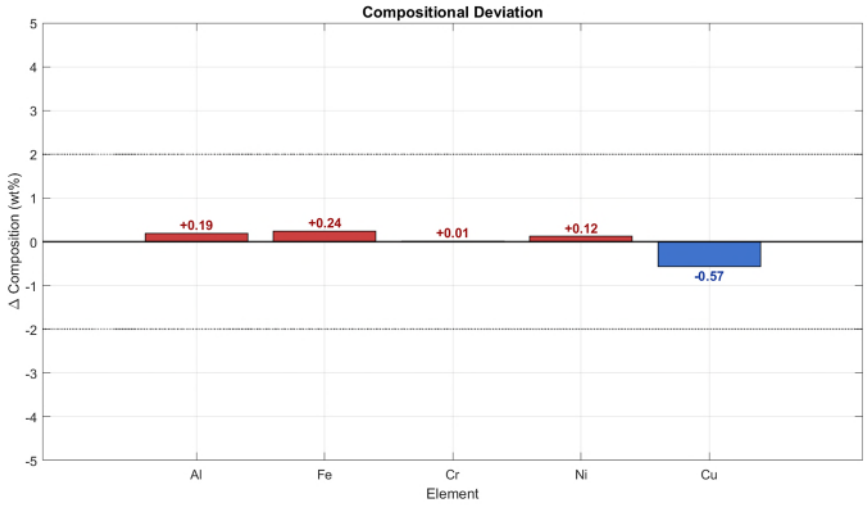


Fig. 9. Element-specific compositional deviations between target and predicted film compositions for the Al-Fe-Cr-Ni-Cu alloy (I8-11). Positive values indicate enrichment and negative values indicate depletion.

3.4 Sputtering Yield — Al-Fe-Cr-Ni-Cu (Fig. 10)

The yield curves for the Al-Fe-Cr-Ni-Cu alloy (Figure 10) retain the racetrack-shape peaks typical for Figure 5 but differ in terms of the material constituting the lowermost curve. Instead of manganese, aluminum is used, which occupies about 0.85 atom per ion position behind Mn due to its relatively small atomic mass and high threshold energy; hence, light materials again prove less prone to erosion by ions in the cascade mode of action. Despite such widening of the whole yield range from Al to Cu, aluminum's very low bulk content (2-4%) makes the effect of aluminum on the sputtering flux relatively small. For the main constituents of the material (Fe, Cr, Ni), the spread of yields is smaller compared to Figure 5, which accounts for the low degree of elemental variations shown in Figures 6-9. Furthermore, owing to the proximity of target edges and consequently higher energy of ions at those positions, the Bohdansky threshold [8] tends to be exceeded more often than in the Fe-Cr-Ni-Mn-Cu alloy.

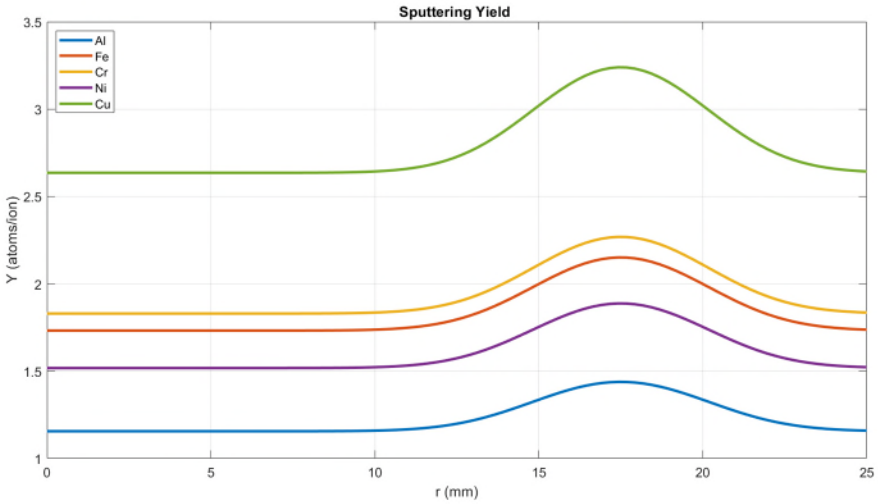


Fig. 10. Radial distribution of element-resolved sputtering yields in the AlFeCrNiCu alloy at 60° ion incidence.

4. Comparison between modelling and experimental results

The results of chemical analyses for the targets obtained by induction melting from selected alloy compositions are presented in Table 1.

Table 1. Chemical composition of the HEA target ingots (wt.%).

Ingot	System	Al	Fe	Cr	Ni	Mn	Cu
I8-6	Fe-Cr-Ni-Mn-Cu	—	23.98	22.08	22.68	26.37	4.90
I8-7	Fe-Cr-Ni-Mn-Cu	—	23.90	20.68	22.19	23.19	10.04
I8-10	Al-Fe-Cr-Ni-Cu	4.21	31.86	28.66	30.86	—	4.41
I8-11	Al-Fe-Cr-Ni-Cu	2.26	45.71	4.51	35.49	—	12.03

The film compositions obtained by simulations (Tables 2–3) has a difference of ±1 wt.% from the target given compositions (dashed lines in Figs. 2, 4, 7, 9), and mass conservation is satisfied throughout. Slightly higher differences are registered by Mn and Cu, but within the acceptable range.

All film values in Table 2 are deterministic model outputs. No sensitivity analysis was performed, and results depend on the assumed Kmc, vapor-pressure, and oxidation parameters. The differences between targets and experimental compositions, and between modelled and experimental data was also presented in table 2. The variation of elemental differences across samples was presented in figure 11.

The modelled film compositions showed good agreement with the experimental values for all the alloys studied. Most of the deviations were less than ±4% by weight, indicating a high degree of accuracy in the predictions provided by the proposed composition calculation model. The measurements performed showed that the model's results are largely correct. Larger differences were observed only in certain cases: for Ni in I8-6, with an increase of +3.44% by weight; for Fe in I8-7, a decrease of −3.51% by weight; for Mn in I8-6 and I8-7 with a variation of -2.18% and2.38%, respectively; and for Cu in I8-11, a decrease of −2.21% by weight. While Ni and Fe can influence the sputtering deposition process due to their ferromagnetic properties, Cu—being a heavier metal—and Mn—having a high vapor pressure—affect the process in different ways. A complex, multiscale model that takes in consideration specific characteristics of various metals ca derive from present calculations. In conclusion, the results show that the model and forms a significant baseline for the simulation of metallic film deposition by DC sputtering method and is applicable for working with complex multi-component alloys.

Table 2. Modelling and experimental element weight percentage and differences for the deposited films versus targets.

Ingot	Element	Target compoz	Modelled film compoz	Experimental film compoz	ΔC_{mod}	ΔC_{exp}	$\Delta C_{mod-exp}$
I8-6	Fe	23.98	24.40	24.35	0.42	0.37	-0.05
	Cr	22.08	22.41	21.39	0.33	-0.69	-1.02
	Ni	22.68	23.05	26.49	0.37	3.81	3.44
	Mn	26.37	25.41	23.23	−0.96	-3.14	-2.18
	Cu	4.90	4.73	4.54	−0.17	-0.36	-0.19

I8-7	Fe	23.90	24.35	20.84	0.45	-3.06	-3.51
	Cr	20.68	21.01	20.14	0.33	-0.54	-0.87
	Ni	22.19	22.57	23.25	0.38	1.06	0.68
	Mn	23.19	22.37	24.75	−0.82	1.56	2.38
	Cu	10.04	9.70	11.02	−0.34	0.98	1.32
I8-10	Al	4.21	4.54	4.42	0.33	0.21	-0.12
	Fe	31.86	31.87	32.32	0.01	0.46	0.45
	Cr	28.66	28.60	27.6	−0.06	-1.06	-1
	Ni	30.86	30.81	31.12	−0.05	0.26	0.31
	Cu	4.41	4.18	4.54	−0.23	0.13	0.36
I8-11	Al	2.26	2.45	1.83	0.19	-0.43	-0.62
	Fe	45.71	45.95	47.34	0.24	1.63	1.39
	Cr	4.51	4.52	4.65	0.01	0.14	0.13
	Ni	35.49	35.61	36.94	0.12	1.45	1.33
	Cu	12.03	11.46	9.25	−0.57	-2.78	-2.21

Table 3. Comparative summary of compositional transfer fidelity metrics for all investigated HEA

	I8-6	**I8-7**	**I8-10**	**I8-11**
System	Fe-Cr-Ni-Mn-Cu	Fe-Cr-Ni-Mn-Cu	Al-Fe-Cr-Ni-Cu	Al-Fe-Cr-Ni-Cu
Max $\|\Delta C_{mod}\|$	0.96 (Mn)	0.82 (Mn)	0.33 (Al)	0.57 (Cu)
Most enriched	Fe (+0.42)	Fe (+0.45)	Al (+0.33)	Fe (+0.24)
Most depleted	Mn (−0.96)	Mn (−0.82)	With (−0.23)	With (−0.57)

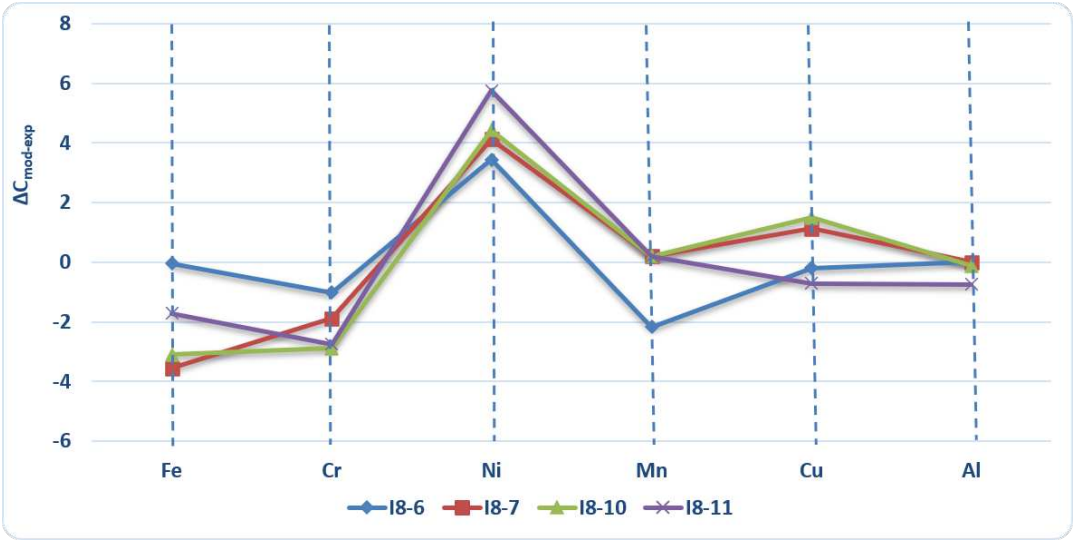


Fig. 11. Elemental variation across various alloy compositions.

5. Conclusions

The model calculations performed for four HEA ingots, all prepared under the same DC magnetron sputtering technique, lead to the following conclusions:

(1) The composition deviations are less pronounced in the case of Al-Fe-Cr-Ni-Cu as compared with Fe-Cr-Ni-Mn-Cu (see Table 3), this is due to the larger effective binding energy.

(2) Copper has the highest yield in both alloys, whereas Ni takes the last place in terms of yields; this trend is defined by the atomic weight, binding energy, and cascade correction coefficients [7], [9].

(3) In Fe-Cr-Ni-Mn-Cu, a change in the Cu/Mn ratio results in a redivision of the deviation budget between these elements without significantly decreasing the calculated transfer reliability.

(4) The difference between target and modelled film compositions falls within a low uncertainty range (±1 wt.%).

(5) the comparison between modelled and experimental values showed a reliable difference of ±4 wt.%, with certain elements that produced the highest values due to their specific properties: Ni and Fe are ferromagnetic, Cu is a heavy metal and Mn has high vapor pressure.

(6) The semi-empirical model presented in the paper needs further improvement, but the comparison results show good capability to simulate the deposition of high entropy alloys by DC sputtering.

Funding
This work was supported by PNRR/2022/C9/MCID/I8, CF58/14.11.2022, contract no. 760105/23.05.2023 (acronym AHEAD) funded by the European Union – Next Generation EU and by a grant of the Ministry of Research, Innovation and Digitization, CNCS/CCCDI – UEFISCDI, project number PN-IV-P6-6.1-CoEx-2024-0162, within PNCDI IV.

Author contributions statement
Conceptualization, L.B. and D.M.; Data curation, L.F.M., M.N.C. and A.S.; Funding acquisition: A.M.M. and L.M.C.; Investigation: L.B., L.F.M. M.N.C. and A.S.; Methodology, L.B., L.F.M., A.O.; Project administration, A.M.M and L.M.C.; Supervision, D.M., and A.O.; Visualization, D.M, L.M.C, and A.S.; Writing—original draft, L.B., A.S., L.F.M.; Writing—review & editing, D.M., L.M.C, A.O. All authors have read and agreed to the published version of the manuscript.

Data availability
The datasets used and/or analysed during the current study are available from the corresponding author on reasonable request.

References

[1] J.-W. Yeh, S.-K. Chen, S.-J. Lin, J.-Y. Gan, T.-S. Chin, T.-T. Shun, C.-H. Tsau, and S.-Y. Chang, "Nanostructured high-entropy alloys with multiple principal elements: Novel alloy design concepts and outcomes," Adv. Eng. Mater., vol. 6, no. 5, pp. 299–303, 2004, doi: doi.org/10.1002/adem.200300567

[2] B. Cantor, I. T. H. Chang, P. Knight, and A. J. B. Vincent, "Microstructural development in equiatomic multicomponent alloys," Mater. Sci. Eng. A, vol. 375–377, pp. 213–218, Jul. 2004, doi: doi.org/10.1016/j.msea.2003.10.257

[3] D. B. Miracle and O. N. Senkov, "A critical review of high entropy alloys and related concepts," Acta Mater., vol. 122, pp. 448–511, Jan. 2017, doi: doi.org/10.1016/j.actamat.2016.08.081

[4] E. P. George, D. Raabe, and R. O. Ritchie, "High-entropy alloys," Nat. Rev. Mater., vol. 4, no. 8, pp. 515–534, Aug. 2019, doi: doi.org/10.1038/s41578-019-0121-4

[5] M. C. Gao, J.-W. Yeh, P. K. Liaw, and Y. Zhang, Eds., High-Entropy Alloys: Fundamentals and Applications, Cham: Springer, 2016, doi: doi.org/10.1007/978-3-319-27013-5

[6] P. Sigmund, "Theory of sputtering. I. Sputtering yield of amorphous and polycrystalline targets," Phys. Rev., vol. 184, no. 2, pp. 383–416, Aug. 1969, doi: doi.org/10.1103/PhysRev.184.383

[7] Y. Yamamura and H. Tawara, "Energy dependence of ion-induced sputtering yields from monatomic solids at normal incidence," At. Data Nucl. Data Tables, vol. 62, no. 2, pp. 149–253, Mar. 1996, doi: doi.org/10.1006/adnd.1996.0005

[8] J. Bohdansky, “A universal relation for the sputtering yield of monatomic solids at normal ion incidence,” Nucl. Instrum. Methods Phys. Res. B, vol. 2, no. 1–3, pp. 587–591, 1984, doi: doi.org/10.1016/0168-583X(84)90271-4

[9] R. Behrisch and W. Eckstein, Eds., Sputtering by Particle Bombardment: Experiments and Computer Calculations from Threshold to MeV Energies, Topics in Appl. Phys., vol. 110. Berlin: Springer, 2007, doi: doi.org/10.1007/978-3-540-44502-9

[10] M. Nastasi, J. W. Mayer, and J. K. Hirvonen, Ion–Solid Interactions: Fundamentals and Applications, Cambridge: Cambridge University Press, 1996, doi: doi.org/10.1017/CBO9780511565007

[11] M. A. Lieberman and A. J. Lichtenberg, Principles of Plasma Discharges and Materials Processing, 2nd ed. Hoboken, NJ: Wiley, 2005, doi: doi.org/10.1002/0471724254

[12] J. A. Thornton, “High rate thick film growth,” Annu. Rev. Mater. Sci., vol. 7, pp. 239–260, 1977, doi: doi.org/10.1146/annurev.ms.07.080177.001323